Agata KOŁODZIEJCZYK[1], Magdalena ŁADNIAK[2], Adam PIÓRKOWSKI[2]

CONSTRUCTING SOFTWARE FOR ANALYSIS OF NEURON, GLIAL AND ENDOTHELIAL CELL NUMBERS AND DENSITY IN HISTOLOGICAL NISSL-STAINED RODENT BRAIN TISSUE

Cell number, density and volume of white and gray matter in brain structures are not constant values. Cellular alterations in brain areas might coincide with neurological and psychiatric pathologies as well as with changes in brain functionality during selection experiments, pharmacological treatment or aging. Several softwares were created to facilitate quantitative analysis of brain tissues, however results obtained from these softwares require multiple manual settings making the computing process complex and time-consuming. This study attempts to establish half automated software for fast, ergonomic and an accurate analysis of cellular density, cell number and cellular surface in morphologically different brain areas: cerebral cortex, pond and cerebellum. Images of brain sections of bank voles stained with standard cresyl-violet technique (Nissl staining), were analyzed in designed software. Results were compared with other commercially available tools regarding number of steps to be done by user and number of parameters possible to measure.

1. INTRODUCTION

The cellular composition of nervous tissue basically consists of three types of cells: neurons, glia and endothelial cells (Fig. 1). Neurons have euchromatin in the nucleus, a clearly visible nucleolus with surrounding cytoplasm. Glial cells have heterochromatin in the nucleus and no cytoplasm. Endothelial cells have a curved shape or are located around blood vessels. With the exception of endothelial cells, the number, density, volume and morphology of these cell populations occurring in pathologies such as schizophrenia or autism, have been extensively discussed during the last years [22], [1], [2], [4], [11], [19], [23], [8], [6]. Post-mortem studies still retain the best method to get information about neuroanatomy of nervous system. Observed morphological changes correlate with changes in brain function. Example, schizophrenia is associated with lower volume of brain structures in cortical regions reflected in lower glial cell number [9], [25], without a change in neuron number [19], [29]. Recent study revealed that neurons of autistic people are much more branched and contain more synapses [28]. Moreover, brain neuroanatomy can be changed after pharmacological treatment. Chronic exposure to

---

[1] Institute of Environmental Sciences, Jagiellonian University.

[2] Department of Geoinfomatics and Applied Computer Science, AGH University of Science and Technology, A. Mickiewicza 30 Av., 30–059 Cracow, Poland, {mladniak,pioro}@agh.edu.pl.

antipsychotic medications like olanzapine and haloperidol results in a significant reduction of brain weight and volume in makaque monkeys [5].

Volumetric measurement of brain structure on brain images is regarded as a gold standard, yet is very time consuming. The simple linear and cross-sectional area measurements are rapid (20 min versus 5 h for volumetric); highly accurate for test-object measurement versus true size; have excellent intraobserver reliability; and, for most brain structures, the simple measures correlated highly significantly with volumetric measures. The simple measures are in general highly reproducible, the difference (as a percentage of the area or width of a region) between the two raters being around 10%, range 0.1% -14.1%, (similar to inter-rater variability in previous studies of volume measurements). The simple linear and area measures are reproducible and correlate well with the measured volumes, and there is a considerable time saving with the former. In circumstances where a large volume of work precludes detailed volume measurement, simple methods are reliable and can be used instead [31].

Cell counting by hand and eye is not practical, if there are many cells per image or many images to process. Counting can be automated, although depending on image, this can get to be complicated process, especially for multi-color images, counts from histology or brightfield image, counting cells within a region, etc. Cell counting via image processing is a common method used in life science labs [7], [24], [20], [26], [14], [27]. Several softwares are comercially available to count cell number, like TIMWIN downloadable from Garbo, SIGMASCAN downloadable from SYSTAT, Image-Pro Plus downloadable from MediaCybernetics, Scion Image from ScionCorp, NIH-Image from NIH, Object Image from Uni Amsterdam, DucoCell Analysis Software from Cellix, DA Cell Counter from Yamato, and Fiji [21]. A free open access software, ImageJ [30], which has possibility to develop a custom counting routine or macro is probably the most widely used for image processing.

Since the results obtained from available softwares require multiple manual settings making the computing process complex and time-consuming, we attempted to establish half automated software for fast, ergonomic and accurate analysis of cellular density, cell number and cellular surface in morphologically different brain areas: cerebral cortex, pond and cerebellum.
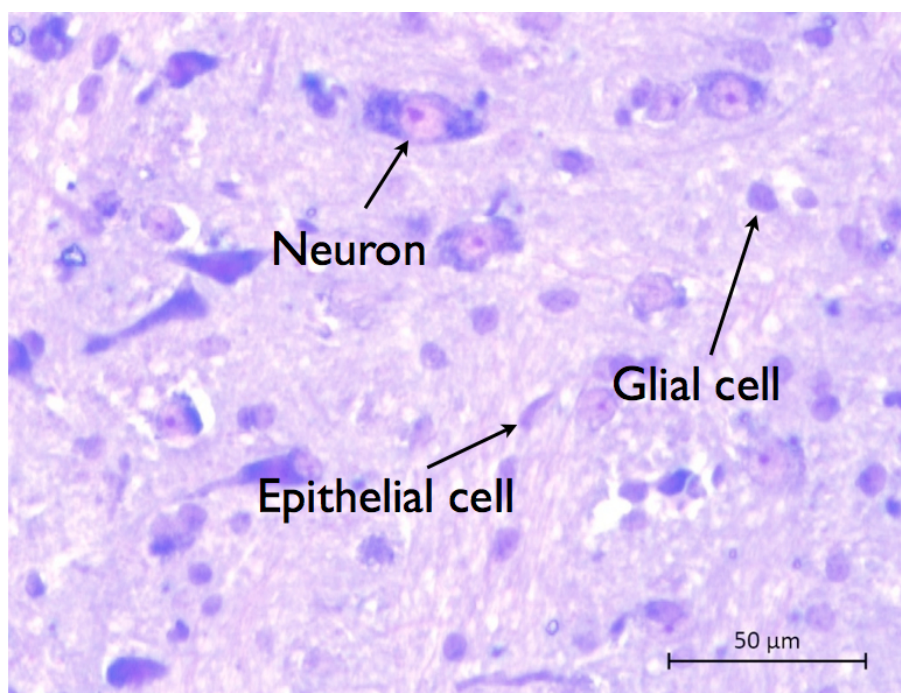

Fig. 1. Morphological criteria for distinguishing neurons, glial and epithelial cells in the nervous tissue stained with standard Nissl staining in the rodent brain.

2. MATERIALS AND METHODS

2.1. ANIMALS

Bank voles (Myodes glaerolus), were taken from the experimental colony of bank voles located in the Institute of Experimental Sciences at the Jagiellonian University. All experimental procedures were compliant with the European Communities Council Directive (2010/63/EU) and were approved by the Animal Care and Use Committee of the Jagiellonian University.

2.2. HISTOLOGY AND IMAGING

Animals were anesthetized with xylazine and ketamine. After transcardial perfusion with 4% PFA (paraformaldehyde in 0.1M phosphate buffer-PB), vole's brains were dissected and fixed overnight in RT (room temperature $21°C$). Brains were washed in 0.1M PB, dehydrated in ethanol and mounted in parafine. 8 micrometre-thick sagittal sections of brain tissues were cut on the Leica microtome and stained with cresyl violet. Images of the brain structures, cerebral cortex, cerebellum and pond were obtained using Zeiss microscope under 40x objective and saved using ZEN software.

2.3. SOFTWARE SPECIFICATION

2.3.1. DETERMINING PARAMETERS OF GRAINS

Determination of cell size requires application of advanced algorithms of computer vision and mathematical morphology. Four types of brain tissues were taken into account: molecular layer and white matter of cerebellum (granular layer of this brain structure is too densely packed with cells for accurate image processing), pond and cerebral cortex (Fig. 2 A-D).

Automatic measurements for image analysis require accurate segmentation. In other words, cells have to be clearly distinguishable from the background [20], [26], what can be obtained by processing transformations of the input image. The application of such operations is presented schematically in the proposed algorithm below (Fig. 3).

2.3.2. PREPROCESSING METHOD - NOISE REDUCTION AND CONTRAST SETTING

The segmentation process started with noise reduction and selection the best sharpened version of the revised input image in RGB colour space. The smallest objects, which did not indicate any cellular voids were removed. The object elimination criterion was established on the basis of the specified magnification of microscopic measurements. The isolated small areas (few pixels in size), were removed by application of 2-D median filtering to simultaneously reduce "salt and pepper" noise (Fig. 4). Each output pixel contained the median value in the m-by-n neighborhood around the corresponding pixel in the input image. To remove measuring noise, morphological filtering "opening and closing" was also performed, with the flat structuring element (SE),which is the 2D matrix on size-dependent noise (about $9×9$ pixels) [24], [20].

Since the algorithm presented on Fig.3. suggests using the image consisting of one colour layer, a one-dimensional grayscale conversion of the image in three-dimensional RGB colour space was performed with pixels located in a numerical range 0-255 according to the conversion formula (Formula I, Tab. 1) [10], [12]. The conversion results are shown in Table 1. In the brain tissue each colour layer carries a different amount of information. The specificity of the test material suggests, that this approach may not be sufficiently effective because of the existence
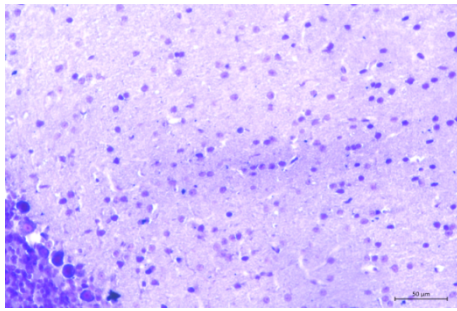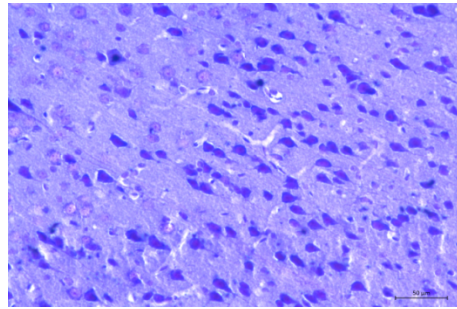
(a) The sagittal section of the molecular layer in cerebellum of bank vole's brain. Left corner of the image reveals a fragment of the granular layer with large Purkinje neurons, which won't be considered in cell counting analysis. Magnification 200x.
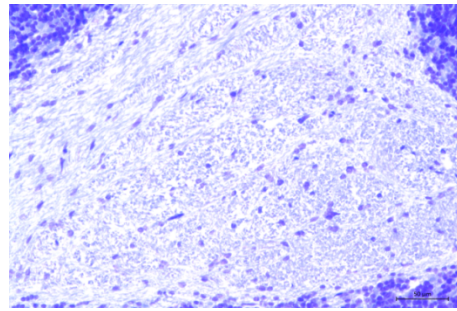
(b) The sagittal section of the cerebellum. Bright area designates the white matter. Magnification 200x.
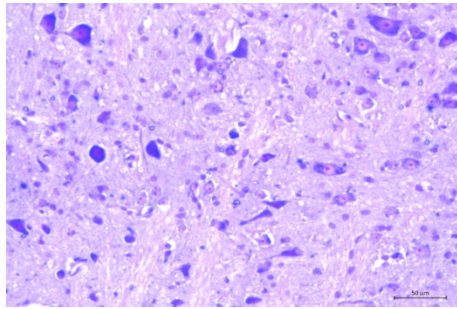
(c) The sagittal section of the pond. Magnification 200x.

(d) The sagittal section of the cerebral cortex. Magnification 200x.
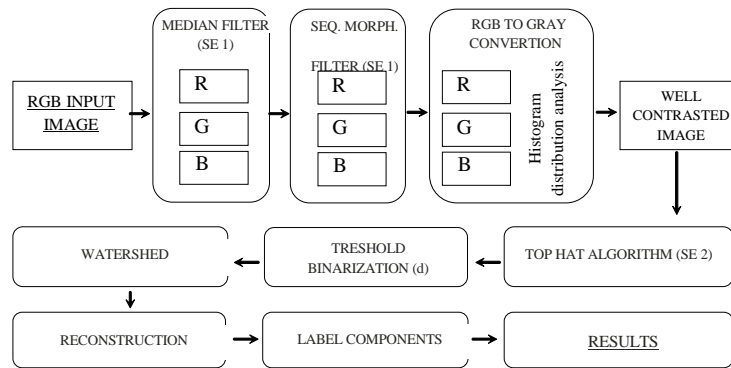
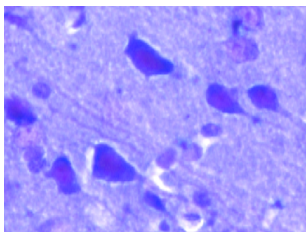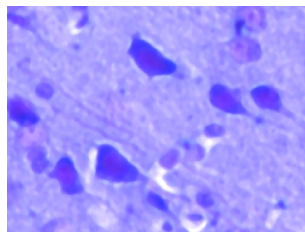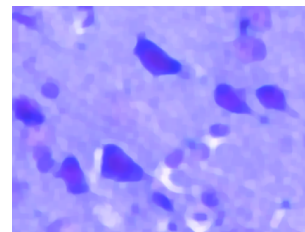Fig. 2.   The materials used for research.

Fig. 3.   The detailed algorithm used in application.

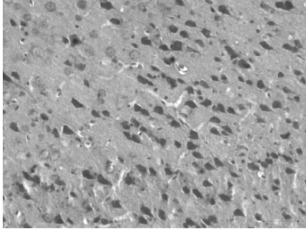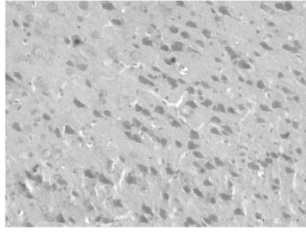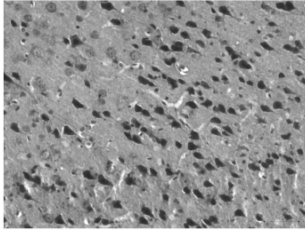(a) Magnification of the part of cortex layer in cerebrum

(b) after noise reduction - median 2D filter

(c) after morphological sequence filter

Fig. 4.   Sample results of using the preprocessing methods.

Table 1. The coefficient of pixels' statistical dispersion and the result of imaging.

Image			
Variance	745.2103	316.1703	1049.4165
RGB Formula (id)	Gray= 0.299*R+0.587*G+0.144*B (I)	0.212*R+0.353*G+0.435*B (II)	Gray=0.00*R+1.00*G+0.00*B (III)

of strongly dominated value. Blue layer has a constant level, which increases the influence of a given feature on the other ones in the process of analysing particular components. To reduce this problem, the Formula I' weight was modified by optimizing proportion of the respective layers to get the greatest output result. Color to greyscale conversion is also relevant in view of futher binarization, color image quality assessment [15] as well as texture similarity estimation [16] affecting the final results.

The image conversion to grayscale was computed with choosing the greatest variance of pixel data. In this inference, the dependent variable was the pixel value for each of the layers of colour and the independent variable was considered as a measure of the variance of the distribution histogram of the image spreading. On this basis of the choice (the best set of colour weights), it the coefficient of statistical dispersion was maximized to obtain a contrasted picture, useful in further analysis (Fig.5(b)).
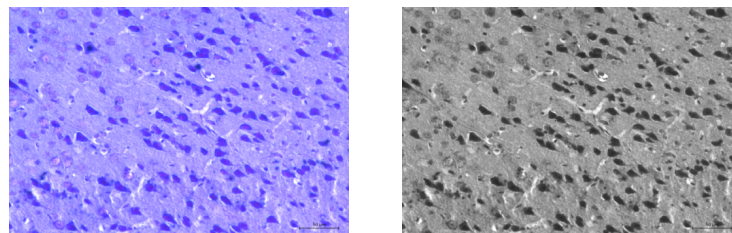
(a) Original input image.　　(b) Input image after preprocessing.

Fig. 5.　The image data after preprocessing methods.

2.3.3. PROCESSING METHODS

The next step was to distinguish cells from the background. After verifying the suitability of many algorithms for filtering the images, like accomplished by means of convolution between a convolution mask and an image, we performed top-hat filtering on an intensity image using a structural element. Top-hat operation in this case was the equivalent of subtracting the result of performing a morphological opening operation on the reversed image from the input image. The flat SE was the 2D square-shaped matrix, where the location of 1's defines the neighbourhood for the morphological operation. The size of the SE was determined the size of the grains in the microscopic image. The analyzed cortex images contain grain size in about 70 pixels, so this size was considered.

The result (Fig. 6(a)) was subjected to binarization with the threshold (Fig. 6(b)) , which can be determined also in a manual or automatically - for instance adaptive methods or methods with as dynamic selection ([18], min. entropy or [17], [3]).

The next stage was morphological filtering - erosion with the SE structural element with size 9. The size of the matrix was determined by the size of the remained after pre noise
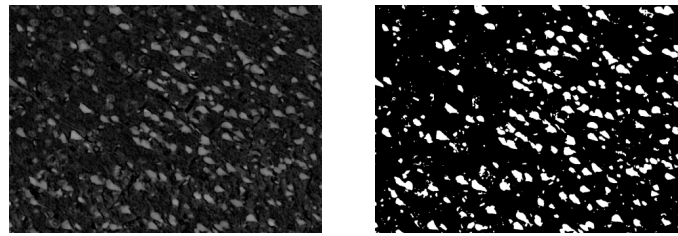
(a) Image (Fig. 5(b)) after Top-Hat transformation.

(b) Image (Fig. 6(a)) after treshold binarization.

Fig. 6.   Sample results of using the processing methods (I).
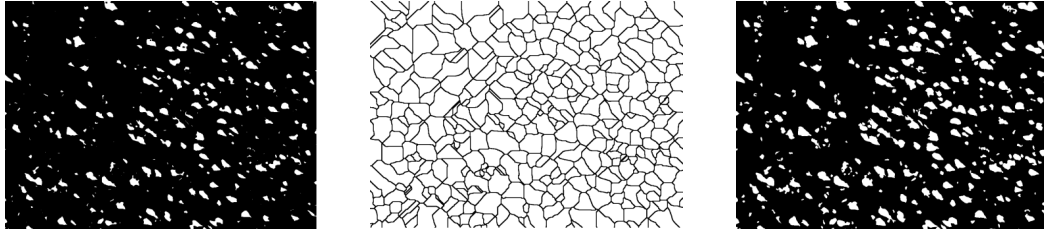

(a) Image (Fig. 6(b)) after erosion.

(b) Image (Fig. 7(a)) after watershed.

(c) Image (Fig. 6(b)) after reconstruction.

Fig. 7.   Sample results of using the processing methods (II).

reduction. The resulting image contains objects combined into one after the transition. Since this phenomenon is common and may lead to incorrect final analysis, we applied the method of watersheds with 8-connected neighborhoods ([26]), which computes a label matrix identifying the watershed regions (Fig. 7(b)) of the input image (Fig.6(b)). The elements labeled 0 mean here the border of the watersheds.

The eroded image underwent reconstruction transformation (Fig. 7(c)) in the image before erosion (Fig. 7(a)). The purpose of this step was to recreate the real size of large objects, which have been reduced as a result of erosion. In order to obtain the final image (Fig. 8(b)), the result of the reconstruction (Fig. 7(c)) was generated from watershed image (Fig. 6(b)). Output image (Fig. 8(b)), was subjected to surgery component label, becoming a starting point for further parameter measurements (Fig. 9).
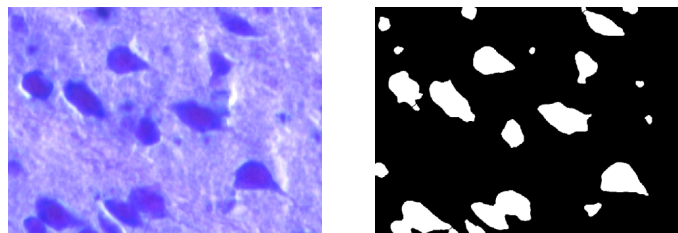
(a) The part of the original input image.

(b) The part of the image after subjection.

Fig. 8.   The image data after processing methods.

3. RESULTS

The application of the proposed solution enabled database construction of selected number of parameters. This can be used in the future in data analysis process, which converts data into usable knowledge. The described measuring methodology was implemented for detection of well contrasted grains in the specimens of nervous tissue in cerebellum, cerebrum and pond.
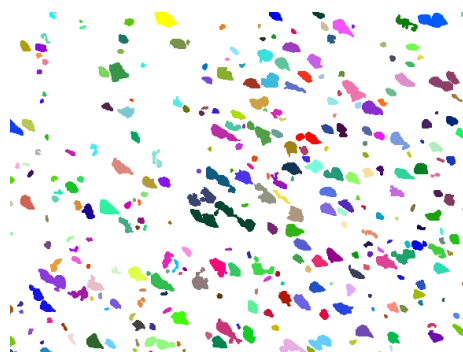
Fig. 9. The image data after labeling method.

Table 2. Measurements of cell number, cell surface area and density.

Figure	proposed method				ImageJ			
	2A	2B	2C	2D	2A	2B	2C	2D
cell number	338	385	528	485	558	451	560	1021
cell surface area	311741	612239	480547	503304	202606	95050	220115	580304
cell density	0.0623	0.1224	0.0961	0.1006	0.0405	0.019	0.044	0.116

Three types of parameters were selected:

- cell number - a number of objects, where the counting process was carried out by using the labelling algorithm consisting on viewing the binarized image line by line until a point belonging to the object. A label and the values of preceding pixels were analyzed. The labeled vertices were based on associativity to neighbour values - three higher and one left neighbour (8-connected neighborhood);
- cell surface area - was calculated by summing all pixels within the object and optionally it may be multiplying by the calibration factor for optimization for image sizes;
- cell density - understood as the cell surface area per total area of the image.

To verify accuracy of the system, the results of the presented method were compared to the results of ImageJ. The authors tried to compare the results with the ITCN (Image-based Tool for Counting Nuclei, ver. 1.6) [13] but there were three parameters, the choice of which was a subjective: cells width, the minimum distance between cells and threshold.

In case of analysing particles in ImageJ, it was very hard to include neurons with light violet nuclei, especially on the Figure 2D, using colour threshold, because cells had their nuclei lighter than the background. Additionally, cytoplasm and cell membranes were not easy to distinguish from the background. The largest disadvantage to measure cells using ImageJ software was small repeatability of threshold settings before binarization process.

4. DISCUSSION AND CONCLUSIONS

The aim of the paper was to present a semi-automatic method of extracting information from digital images about the cell number, density and volume of white and gray matter in brain structures, based on image processing, image analysis and mathematical morphology methods. It was also described the characteristics of images to choose optimal segmentation algorithm. Authors considered the advantages and possibilities of applying mixture weight model of conversion formulas RGB, to obtain the best amount of information. The usefulness of applying the classical algorithms processing and the analysis of digital images (eg. top-hat transformation, watershed, labelling) for the presented data was presented. It was made a general comparison of the proposed method with the popular tools used for semi-automatic statistical evaluation of cells (such as ImageJ). The results of the programs are relatively divergent, because of the

great dependence on the parameters (in the case of an ITCN), which adopts them subjectively. A proof that there is a strong need for methods that perform fully automated segmentation of nerve cells and evaluate the parameters without user intervention. These parameters should take into consideration, together with parameters like shape or anisotropy of different types of cells in the nervous tissue: neurons, glial cells and epithelial cells. This became the subject of further study.

ACKNOWLEDGEMENT

BIBLIOGRAPHY

[1] BERRETTA S., PANTAZOPOULOS H., LANGE N. Neuron numbers and volume of the amygdala in subjects diagnosed with bipolar disorder or schizophrenia. In *Biological psychiatry*, 2007, Vol. 62. Elsevier, pp. 884–893.

[2] BEZCHLIBNYK Y. B., SUN X., WANG J.-F., MACQUEEN G. M., MCEWEN B. S., YOUNG L. T. Neuron somal size is decreased in the lateral amygdalar nucleus of subjects with bipolar disorder. 2007, Vol. 32. Canadian Medical Association, p. 203.

[3] BIELECKA M., PIÓRKOWSKI A. Adaptive preprocessing of x-ray hand images. In *Information Technologies in Biomedicine, Volume 3*, 2014. Springer, pp. 61–70.

[4] BOWLEY M. P., DREVETS W. C., ÖNGÜR D., PRICE J. L. Low glial numbers in the amygdala in major depressive disorder. 2002, Vol. 52. Elsevier, pp. 404–412.

[5] DORPH-PETERSEN K.-A., PIERRI J. N., PEREL J. M., SUN Z., SAMPSON A. R., LEWIS D. A. The influence of chronic exposure to antipsychotic medications on brain size before and after tissue fixation: a comparison of haloperidol and olanzapine in macaque monkeys. 2005, Vol. 30. Nature Publishing Group, pp. 1649–1661.

[6] GARCÍA-AMADO M., PRENSA L. Stereological analysis of neuron, glial and endothelial cell numbers in the human amygdaloid complex. 2012, Vol. 7. Public Library of Science, p. e38692.

[7] GONZALEZ R., WINTZ P. Digital image processing. 1987. Addison Wesley.

[8] HAMIDI M., DREVETS W. C., PRICE J. L. Glial reduction in amygdala in major depressive disorder is due to oligodendrocytes. 2004, Vol. 55. Elsevier, pp. 563–569.

[9] HOF P. R., HAROUTUNIAN V., FRIEDRICH JR V. L., BYNE W., BUITRON C., PERL D. P., DAVIS K. L. Loss and altered spatial distribution of oligodendrocytes in the superior frontal gyrus in schizophrenia. 2003, Vol. 53. Elsevier, pp. 1075–1085.

[10] JI Y., LIU H.-B., WANG X.-K., TANG Y.-Y. Color transfer to greyscale images using texture spectrum. In *Machine Learning and Cybernetics, 2004. Proceedings of 2004 International Conference on*, 2004, Vol. 7. pp. 4057–4061.

[11] KRECZMANSKI P., HEINSEN H., MANTUA V., WOLTERSDORF F., MASSON T., ULFIG N., SCHMIDT-KASTNER R., KORR H., STEINBUSCH H. W., HOF P. R., ET AL. Volume, neuron density and total neuron number in five subcortical regions in schizophrenia. 2007, Vol. 130. Oxford Univ Press, pp. 678–692.

[12] KUMAR T., VERMA K. A theory based on conversion of rgb image to gray image. 2010, Vol. 7. Citeseer, pp. 7–10.

[13] KUO T., BYUN J. ITCN (Image-based Tool for Counting Nuclei).

[14] MŁYNARCZUK M. Description and classification of rock surfaces by means of laser profilometry and mathematical morphology. 2010, Vol. 47. Elsevier, pp. 138–149.

[15] OKARMA K. A validation of combined metrics for color image quality assessment. In *Computer Vision and Graphics*, L. J. Chmielewski, R. Kozera, B.-S. Shin, and K. Wojciechowski, Eds., 2014, Vol. 8671 of *Lecture Notes in Computer Science*. Springer International Publishing Switzerland, pp. 1–8.

[16] OKARMA K., FREJLICHOWSKI D., CZAPIEWSKI P., FORCZMASKI P., HOFMAN R. Similarity estimation of textile materials based on image quality assessment methods. In *Computer Vision and Graphics*, L. J. Chmielewski, R. Kozera, B.-S. Shin, and K. Wojciechowski, Eds., 2014, Vol. 8671 of *Lecture Notes in Computer Science*. Springer International Publishing Switzerland, pp. 478–485.

[17] OSZUTOWSKA-MAZUREK D., MAZUREK P., SYCZ K., WAKER-WÓJCIUK G. Adaptive windowed threshold for box counting algorithm in cytoscreening applications. In *Image Processing and Communications Challenges 5*, 2014. Springer, pp. 3–12.

[18] OTSU N. A Threshold Selection Method from Gray-level Histograms. 1979, Vol. 9. pp. 62–66.

[19] PAKKENBERG B. Pronounced reduction of total neuron number in mediodorsal thalamic nucleus and nucleus accumbens in schizophrenics. 1990, Vol. 47. American Medical Association, pp. 1023–1028.

[20] RUSS J. The image processing handbook. 1992. CRC Press.

[21] SCHINDELIN J., ARGANDA-CARRERAS I., FRISE E., KAYNIG V., LONGAIR M., PIETZSCH T., PREIBISCH S., RUEDEN C., SAALFELD S., SCHMID B., ET AL. Fiji: an open-source platform for biological-image analysis. 2012, Vol. 9. Nature Publishing Group, pp. 676–682.

[22] SCHUMANN C. M., AMARAL D. G. Stereological estimation of the number of neurons in the human amygdaloid complex. 2005, Vol. 491. Wiley Online Library, pp. 320–329.

[23] SCHUMANN C. M., AMARAL D. G. Stereological analysis of amygdala neuron number in autism. 2006, Vol. 26. Soc Neuroscience, pp. 7674–7679.

[24] SERRA J. Image analysis and mathematical morphology, v. 1. 1982. Academic press.

[25] STARK A. K., UYLINGS H. B., SANZ-ARIGITA E., PAKKENBERG B. Glial cell loss in the anterior cingulate cortex, a subregion of the prefrontal cortex, in subjects with schizophrenia. 2004, Vol. 161. Am Psychiatric Assoc, pp. 882–888.

[26] TADEUSIEWICZ R., KOROHODA P. Komputerowa analiza i przetwarzanie obrazów. 1997. Wydawnictwo Fundacji Postępu Telekomunikacji.

[27] TADEUSIEWICZ R., OGIELA M. R. Medical image understanding technology. 2004. Springer, Heidelberg.

[28] TANG G., GUDSNUK K., KUO S.-H., COTRINA M. L., ROSOKLIJA G., SOSUNOV A., SONDERS M. S., KANTER E., CASTAGNA C., YAMAMOTO A., ET AL. Loss of mtor-dependent macroautophagy causes autistic-like synaptic pruning deficits. 2014. Elsevier.

[29] THUNE J. J., UYLINGS H., PAKKENBERG B. No deficit in total number of neurons in the prefrontal cortex in schizophrenics. 2001, Vol. 35. Elsevier, pp. 15–21.

[30] VERARDO M., LEWIS G., TAKEDA M., WARDAK B., RABENA M., CHEN D., FISHER S. Glial hypertrophy and neuronal remodeling in mice deficient in gfap and vimentin following experimental retinal detachment. 2005, Vol. 46. ARVO, p. 2443.

[31] WHALLEY H., WARDLAW J. Accuracy and reproducibility of simple cross-sectional linear and area measurements of brain structures and their comparison with volume measurements. 2001, Vol. 43. Springer, pp. 263–271.